

Generalizing 6-DoF Grasp Detection via Domain Prior Knowledge

Haoxiang Ma^{1,2} Modi Shi^{1,2} Boyang Gao^{3,4} Di Huang^{1,2*}

¹State Key Laboratory of Software Development Environment, Beihang University, Beijing, China

²School of Computer Science and Engineering, Beihang University, Beijing, China

³School of Computer Science and Technology, Harbin Institute of Technology, Harbin, China

⁴Geometry Robotics

{mahaoxiang822, modishi, dhuang}@buaa.edu.cn, {boyang.gao}@geometryrobot.com

Abstract

We focus on the generalization ability of the 6-DoF grasp detection method in this paper. While learning-based grasp detection methods can predict grasp poses for unseen objects using the grasp distribution learned from the training set, they often exhibit a significant performance drop when encountering objects with diverse shapes and structures. To enhance the grasp detection methods' generalization ability, we incorporate domain prior knowledge of robotic grasping, enabling better adaptation to objects with significant shape and structure differences. More specifically, we employ the physical constraint regularization during the training phase to guide the model towards predicting grasps that comply with the physical rule on grasping. For the unstable grasp poses predicted on novel objects, we design a contact-score joint optimization using the projection contact map to refine these poses in cluttered scenarios. Extensive experiments conducted on the GraspNet-1billion benchmark demonstrate a substantial performance gain on the novel object set and the real-world grasping experiments also demonstrate the effectiveness of our generalizing 6-DoF grasp detection method. Code is available at <https://github.com/mahaoxiang822/Generalizing-Grasp>.

1. Introduction

Given an object, robotic grasp detection aims to find suitable and sufficient gripper configurations for various manipulation tasks. Traditional methods [6, 27, 30] establish hand-crafted criteria to evaluate grasp samples according to 3D models of objects. Despite providing precise interaction between objects and grippers, they assume that object models are available in advance and also suffer a slow running speed, which limits their popularization. As the develop-

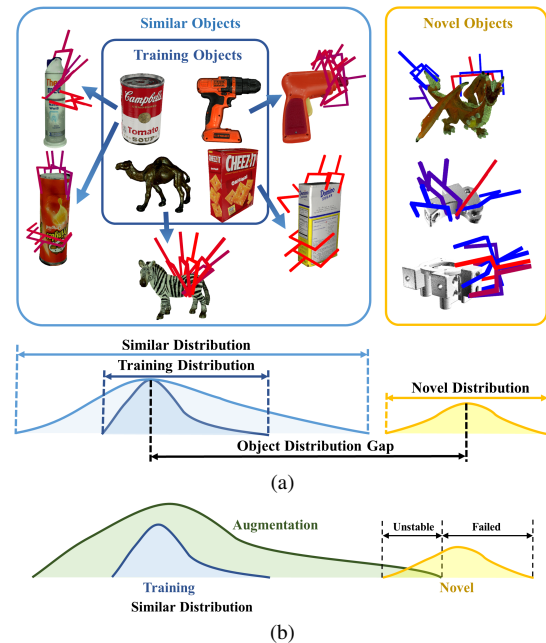


Figure 1. Illustration of (a) the performance and distribution gap between objects similar to training samples (**similar objects**) and those with largely varied shapes and structures (**novel objects**) and (b) the limitations of the object augmentation methods.

ment of deep learning, data-driven methods [9, 20, 32] have been widely studied. These methods predict grasps without the need for pre-prepared 3D models and demonstrate the capability to handle unseen objects. However, they often struggle when encountering objects whose shapes and structures significantly deviate from those in the training set, making them difficult to adapt to more diverse applications. As illustrated in Fig. 1 (a), learning-based grasp detection methods are basically able to transfer to objects similar to those appearing in training, but they do not effectively generalize to novel objects with their distribution greatly changed.

To facilitate the generalization of learning-based grasp

*Corresponding author.

detection methods towards a variety of unseen objects, previous attempts usually apply data augmentation techniques to expand the distribution of the training set. More objects are typically produced by randomly concatenating a number of 3D primitives [1, 33] or by directly synthesizing through generative networks [13, 23]. They do enrich the diversity of objects for training, which leads to a gain in overall performance. However, since such augmentation is conducted only according to original data, it contributes more to similar objects whose distribution is largely overlapped and offers little help to new objects whose distribution is not well covered. As depicted in Fig. 1 (b), on the one hand, to the objects that are far from the center of training samples in the feature space, totally wrong grasps could be delivered. On the other hand, for the ones that are near the center of training samples in the feature space, although reasonable grasps may be obtained, the predictions tend to be unstable due to the distribution gap. Both cases make those methods problematic to generalize to unseen targets.

To address the dilemma above, inspired by informed machine learning [15, 34], we introduce domain prior knowledge of robotic grasping. Compared to data augmentation, domain prior knowledge does not depend on the distribution of training data, allowing for easy adaptation to objects with significant shape and structure differences. Firstly, to enable the grasp detection network to generalize to novel objects, we incorporate certain physical rules on grasping, such as force conditions [26] and contact positions, which are typically used in the traditional analytical grasping methods. The physical rules provide valuable clues in terms of grasp stability regardless of object-specific properties, thus motivating us to integrate such rule-based priors into the grasp detection network. Secondly, to deal with the unstable results predicted by the network, we introduce another type of knowledge about the interaction of the gripper and object. The contact map [2] is able to denote the regions correlated with grasping as well as the kinematics of the gripper. By employing a neural network to encode the preferred object regions for optimal grasps, the learning-based contact map prior can be utilized to refine insufficiently accurate grasps.

Concretely, in this paper, we propose a generalized 6-DoF grasp detection framework with domain prior knowledge, which consists of two components: Physical Constraint Regularization (**PCR**) and Contact-Score Joint Optimization (**C-SJO**). In PCR, we integrate the physical prior into the network as the regularization, thereby constraining the correlation between gripper poses and object models. To enable the back-propagation of PCR, we employ an end-to-end 6-DoF grasp detection network for grasp prediction and utilize the Signed Distance Field (SDF) to encode the object model, facilitating the differentiable computation of physical constraints. Compared to fitting grasp annotations directly, PCR guides the network to predict grasps follow-

ing object-independent physical rules, thereby enhancing the generalization capability for novel objects. To refine the unstable prediction for novel objects, we introduce the C-SJO at test time based on the contact map prior. The contact map represents the contact region on the object’s surface by calculating the distance between the gripper model and the objects. A contact map prediction network is introduced to encode the contact pattern of good grasps by learning from grasp labels. By aligning the contact map of the current grasp and the prediction from the network, the grasp pose can be optimized within its neighborhood. However, as for 6-DoF grasp detection in clutter, using the euclidean distance for contact map calculation cannot adequately address inaccurate contact positions. Therefore, we introduce a projection contact map to solve this problem. Additionally, due to the noise from the depth sensor and the occlusion in cluttered scenarios, relying solely on the contact prior can lead to singular results. To mitigate this, we use score optimization to constrain the searching space of contact optimization, in which a grasp score network is utilized.

The contribution of this paper can be summarized as:

- We propose a domain prior knowledge informed 6-DoF grasp detection framework to enhance the generalization ability for novel objects.
- We design the physical constraint regularization to represent the physical prior for 6-DoF grasping and integrate it into the network in a differential strategy.
- We employ a contact-score joint optimization with the projection contact map, which is suitable for refining the inaccurate prediction in cluttered scenarios.

2. Related work

6-DoF Grasp Detection To generate diverse and feasible grasping in cluttered scenes, 6-DoF grasp detection has been advanced recently. Compared to planar grasp detection where the grasp space is limited [9, 22, 28], 6-DoF grasp detection method can predict grasping in $SE(3)$ space, thereby supporting more complex downstream task. [32] pioneers a sampling and evaluation framework for 6-DoF grasp detection. Using point-cloud input, they heuristically sample grasp candidates and employ a Convolutional Neural Network (CNN) for scoring them. [16] build upon the framework, utilizing a neural network for point-cloud data to achieve improved grasp sample evaluation. More recently, a series of studies [3, 8, 10, 14, 19, 24, 29, 35] propose end-to-end strategy for grasp prediction. [24] employs a variational auto-encoder for grasp generation given the object point-clouds. [29] introduces a single-shot grasp proposal network for efficient grasp detection based on single view point-clouds, and [3] employs a Truncated Signed Distance Function (TSDF) to map multiple frames and predict grasps in voxel space. [10] provides a large benchmark

with densely annotated grasp labels and designs a baseline method for dense grasp prediction. Subsequently, [35] defines graspness to represent grasp probability in searching space and [19] focuses on the scale imbalance problem for 6-DoF grasp detection. With the development of neural representations, [14] utilizes an occupancy network to learn a shared representation between 3D reconstruction and grasp detection. [8] introduces a generalizable neural radiance field for the grasp detection of transparent and specular objects. Despite these advancements in 6-DoF grasp detection, the performance for novel objects, particularly those with varied shapes and structures, remains sub-optimal. In this paper, we investigate this shortcoming.

Generalization on Grasp Detection Several strategies are proposed to enhance the generalization capability of grasp detection, which mainly focuses on enriching the distribution of training objects. [1] procedurally generates objects by attaching rectangular prisms at random locations and orientations. To enhance the shape diversity, [33] constructs a set of object primitives by decomposing everyday objects and generates diverse objects by randomly sampling these primitives and combing them. In addition to heuristically generating random objects, [23] provides the Evolved Grasping Analysis Dataset (EGAD), which includes objects of varying shape complexity and grasp difficulty generated by the 3D compositional pattern producing networks. [13] employs an AutoEncoder-Critic network to interpolate new shapes from two objects for augmentation. Besides augmenting current shapes to improve the performance of the learning-based grasp detection method, [36] explores the task of generating adversarial objects that are difficult to grasp. Different from previous augmentation methods for generalized grasp detection, we introduce the grasp domain knowledge to our framework explicitly. Therefore, our method doesn't rely on the distribution of training objects, resulting in an improvement for out-of-distribution objects.

Usage of domain knowledge in Grasping Domain prior knowledge has been leveraged in various grasping applications. Early analytical methods [11, 21, 31] make use of the physical prior knowledge to examine the force dynamics between the gripper and the object. More recently, several methods incorporate some grasp prior knowledge into the hand-object grasp synthesis. [18] introduces a differentiable force closure algorithm designed to optimize hand configurations, which facilitates the fast generation of physically stable grasps. [17] designs a generalized Q1 metric that serves as a loss for a grasp planner, producing precise multi-finger grasping for single object with watertight model or rendered depth images. While the aforementioned methods employ domain prior knowledge to assist grasp synthesis and optimization, they rely on the accurate object shapes and design complex calculations for prior integration. This makes it difficult to apply them in the 6-DoF grasp detection

where the generation of diverse grasps in complex scenarios is required and the object geometry from the depth sensor is inaccurate.

3. Method

3.1. Physical Constraint Regularization

In terms of physical prior knowledge, the force interaction between the object and the gripper is used to analyze grasp stability, among which the force closure [26] is widely adopted. A force closure grasp can resist any external wrenches with the contact force if the force direction lies in the friction cone. In scenarios where the friction coefficient of the object surface is unknown and a two-finger gripper is utilized, we employ the antipodal rule [5] as a simplification. Given two contact points (u_1, u_2) lying on the object surface, the antipodal rule is formulated as:

$$[p(u_1) - p(u_2)] \cdot t(u_1) = 0 \quad (1)$$

$$[p(u_2) - p(u_1)] \cdot t(u_2) = 0 \quad (2)$$

$$n(u_1) + n(u_2) = 0 \quad (3)$$

where $p(u)$ represents the contact position, $t(u)$ represents the unit tangent vector and $n(u)$ represents the unit outward normal vector. If the contact points (u_1, u_2) between the gripper and the object comply with the antipodal rule, there is a higher probability of a successful grasp. Based on which, we introduce the PCR to constrain the output of the network with the rule.

With the predicted grasp pose $g = [t, R, w]$ and the gripper kinematic model K , the gripper contacts (c_1, c_2) can be expressed as:

$$(c_1, c_2) = K(t, R, w) \quad (4)$$

To enforce the gripper contacts to comply with the antipodal constraint, we propose an antipodal regularization term, which is calculated as follows:

$$R^A(c_1, c_2) = 1 - 0.5 * (\cos(\overrightarrow{c_1 c_2}, n(c_2)) + \cos(\overrightarrow{c_2 c_1}, n(c_1))) \quad (5)$$

where $\overrightarrow{c_1 c_2}$ is the vector connecting the gripper's contact points c_1 and c_2 , $n(c_1)$ and $n(c_2)$ are the normal vectors at the respective contact points and \cos represents the cosine similarity. Nevertheless, the predicted gripper contacts c_1, c_2 may not lie precisely on the object surface. To overcome this, we also introduce constraints on the distance between the gripper contacts and the object's surface. These constraints help to avoid collision and ensure that the contact points are sufficiently close to the object's surface. The collision constraint R^C and surface constraint R^S are formulated as:

$$R^C(c_1, c_2) = \text{Max}(0, \theta - d(c_1)) + \text{Max}(0, \theta - d(c_2)) \quad (6)$$

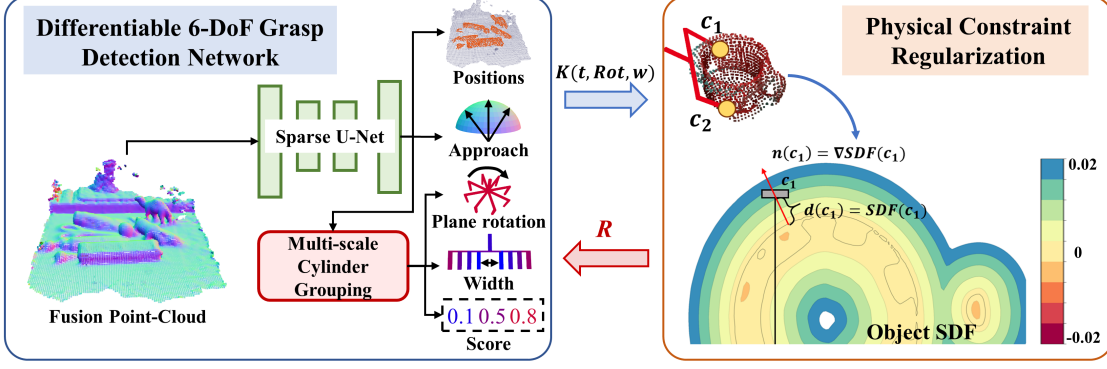


Figure 2. The pipeline of differential physical constraint integration. With the fusion point-cloud, the differentiable 6-DoF grasp network predicts the grasp configurations. The position of contacts c_1, c_2 are calculated from grasp configurations by the gripper model and the regularization R is computed from the object SDF for back-propagation.

$$R^S(c_1, c_2) = \text{Max}(0, d(c_1) - \mu) + \text{Max}(0, d(c_2) - \mu) \quad (7)$$

where the contact distance $d(c)$ is constrained between $[\theta, \mu]$. Besides, we use the grasp score predicted by the grasp detection network to weight the regularization of different grasps, thereby ensuring the coherence between the grasp score and the physical constraints. With the grasp score of i th grasp s_i , the overall physical constraint R_i can be represented as:

$$R_i = \frac{s_i * (R_i^A + R_i^C + R_i^S)}{\frac{1}{M} \sum_j s_j} \quad (8)$$

where M is the number of seed points. The overall loss L can be formulated as:

$$L = L_{grasp} + \phi * R \quad (9)$$

For more details of the grasp configuration loss L_{grasp} , please refer to the supplementary.

3.2. Differential Physical Constraint Integration

To integrate the PCR into the grasp detection network, the sub-gradients of normal vector $\frac{\partial n(c)}{\partial c}$ and surface distance $\frac{\partial d(c)}{\partial c}$ with respect to the contact point c should be computed. Besides, the generation of grasp poses should be differential. As a result, we introduce an end-to-end 6-DoF grasp network and the differentiable Signed Distance Function (SDF) for the calculation of PCR. As shown in Fig. 2, the configurations of the gripper are regressed from the input fusion point-cloud in an end-to-end manner. With the configurations predicted by the grasp detection network, the contact point c can be calculated by the gripper kinematics model. Utilizing SDF of the object, we can query the surface distance of the contact c_1 directly by $d(c_1) = SDF(c_1)$ and the normal vector of c_1 can be calculated by $n(c_1) = \nabla SDF(c_1)$. In practice, obtaining an

object's SDF directly is not feasible. Consequently, we employ a 3D grid to represent the object's SDF, where each grid point records the corresponding SDF value. During training, the SDF value at any arbitrary position is computed using tri-linear interpolation, which allows for the differentiable computation of the gradients required by the physical constraints.

3.3. Contact-Score Joint Optimization

Due to the significant discrepancy in shape and structure between novel and training objects, the grasp prediction from the network can be unstable, which leads to failures. To solve this problem, inspired by dexterous grasp synthesis [12, 37], we introduce the contact map prior which encodes the preference contact region on the object to refine inaccurate grasps. Given the object point-cloud X_o and gripper contacts c_1, c_2 , we define the contact map of each point $p_i \in X_o$ for a 6-DoF grasp as:

$$D_i = \min_j \| p_i - c_j \|, c_j \in \{c_1, c_2\} \quad (10)$$

Compared with optimization for a single object with accurate geometry in grasp synthesis, for the 6-DoF grasp detection task in cluttered scenes, there exist two issues that make the test-time optimization impractical and cause singular results: (1) the contact points don't always lie on the object surface; (2) the object point-clouds in real-world scenarios are inaccurate and incomplete. For the first issue, we propose the projection contact distance PD illustrated in Fig. 3 (a) as a supplementary of original contact distance D , which calculates the projection distance from the object point-cloud to the connecting line of two contacts.

$$PD_i = D_i * \sin(\theta_i) \quad (11)$$

We visualize the original contact map and the proposed projection contact map in Fig. 3 (b). Rather than computing the contact distance directly, the projection contact

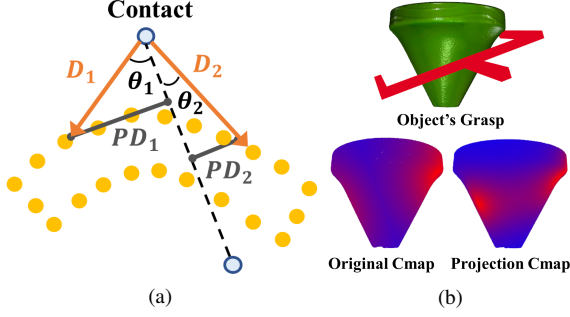


Figure 3. (a) Calculation of the contact map and (b) comparison of the projection contact map and the original version.

map can highlight the accurate contact region on the object point-cloud for coarse grasp poses whose contact points may not lie on the surface. For contact map optimization, as shown in Fig. 4 (a), we employ a ContactNet for contact map prediction, which encodes the contact prior. Given the object point-cloud X_o , the gripper point-cloud X_g and the predicted grasp pose g , the ContactNet can be formulated as:

$$\hat{D}, \hat{PD} = \text{ContactNet}(gX_g, X_o) \quad (12)$$

and thus the contact optimization target J_c is formulated as:

$$J_c = |D - \hat{D}| + \alpha * |PD - \hat{PD}| \quad (13)$$

For the second issue, we incorporate an independent grasp score network ScoreNet in the optimization process as shown in Fig. 4 (b). Trained with the noisy object point-cloud and its corresponding grasp pose sampled from grasp labels, the ScoreNet predicts the grasp score \hat{S} . We sample both the good and bad quality grasps so the ScoreNet can give a low score when the failed grasp appears in the optimization. To suppress the decline in grasp score, the target of score optimization J_s and the overall optimization target J are formulated as:

$$J_s = T - \min(T, \hat{S}) \quad (14)$$

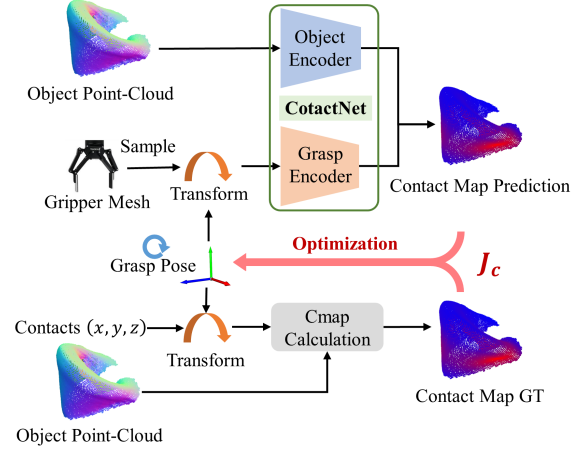
$$J = J_c + \beta * J_s + \gamma * \Delta t \quad (15)$$

where T is the max grasp score, β is the weight of J_s and Δt constrains the offset of position t during optimization. During inference, we adopt an Adam optimizer to optimize the grasp pose iteratively by minimizing J in a gradient descent strategy.

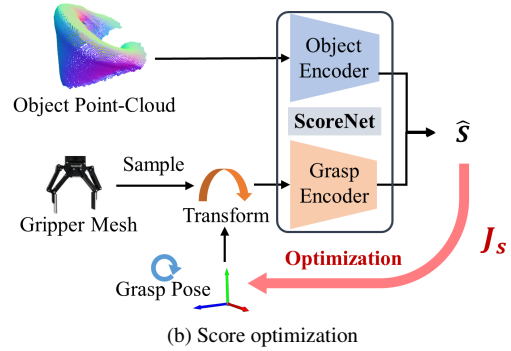
4. Experiments

4.1. Implementation Details

Benchmark We conduct all the simulation experiments on the large-scale GraspNet-1billion benchmark [10]. The benchmark includes 190 cluttered scenes, in which 100 scenes for training, 90 for testing. The testing set is divided



(a) Contact optimization



(b) Score optimization

Figure 4. The pipeline of contact optimization and score optimization with ContactNet and ScoreNet.

into seen, similar and novel set based on the objects in the scenes. Each scene includes 256 RGB-D images captured from different views with RealSense/Kinect cameras. Most previous methods on the benchmark utilize single-view data for training and evaluation. However, the depth images captured from a single view suffer from significant noise. For novel object grasping, as the model has no prior about the objects, it is unable to infer the shape of occluded parts based solely on partial point-clouds, thereby hindering the grasp detection for novel objects. To bypass the interference caused by incomplete point clouds and enhance the capability of grasp detection on novel objects, we reconstruct the depth images from multiple views in a single scene into Truncated Signed Distance Function (TSDF) via KinectFusion [25]. The TSDFs are used for training and evaluation.

Metric We follow the metric used in GraspNet-1billion benchmark [10], in which the average precision of top- k ranked grasps in a scene is considered. In the original metric, k is set to 50, and a maximum of 10 grasps per-object are used for evaluation. Given that most scenes contain around 9 objects, this metric can overlook the grasping accuracy of some objects. Therefore, we employ an object-balanced metric for reconstructed scenes, where $k = N_{object} * 5$.

Model	Seen			Similar			Novel		
	AP	AP _{0.8}	AP _{0.4}	AP	AP _{0.8}	AP _{0.4}	AP	AP _{0.8}	AP _{0.4}
Baseline	<u>66.09</u>	<u>75.57</u>	60.63	64.82	74.10	<u>61.51</u>	30.61	37.61	17.06
+ PCR	66.67	75.67	61.84	65.55	74.42	61.47	35.58	43.49	<u>19.70</u>
w/o R^A	65.63	74.59	<u>61.19</u>	<u>65.38</u>	<u>74.29</u>	62.10	32.38	39.04	18.88
w/o R^C	65.27	75.05	58.62	62.25	71.65	57.11	32.34	38.58	19.27
w/o R^S	63.51	72.37	60.26	64.31	73.00	61.06	<u>35.57</u>	<u>42.60</u>	20.45

Table 1. Results of PCR on scenes captured by RealSense.

N_{object} is the number of objects of the scene and a maximum of 5 grasps per-object are used for evaluation. This provides a more balanced consideration of the grasping accuracy across different objects compared to the original evaluation metrics. AP_μ is employed as the metric, which represents the average $Precision@m$ for m ranges from 1 to m with friction μ . AP is calculated by the average of AP_μ , where μ ranges from 0.2 to 1.2 with the interval $\Delta\mu = 0.2$.

Model implementations We first introduce a strong baseline model based on the scale balanced 6-DoF grasp detection network [19] and GSNet [35]. Following [35], we employ a sparse UNet based on Minkowski Engine [7] as the backbone and calculate the "graspness" for each point to generate grasp candidates. For local feature extraction, the multi-scale cylinder grouping proposed in [19] is employed to improve the performance of the baseline model. For the PCR during training, θ and μ which control the contact distance are set to 0.02 and 0.005 separately and the weight ϕ for the regularization is set to 0.1. For the C-SJO, we set the hyper-parameter $\alpha = 0.2$, $\beta = 0.01$ and $\gamma = 5$.

4.2. Results on Physical Constraint Regularization

We show the results of PCR in Table 1. Compared to the baseline model, integrating the PCR delivers an improvement of 4.64% on the novel set, demonstrating its effectiveness for objects with diverse shapes and structures. Besides, the PCR also improves by 0.58% in seen set and 0.73% in similar set. This illustrates that for seen and similar objects in the training set, introducing physical prior can help the grasp detection network to fully utilize the grasp labels compared to fitting them directly. We also ablate the influence of different physical constraints and notice that the incomplete constraint conditions can attribute to the performance decline on seen and similar set. Only with partial constraints during training, not all the grasp poses which meet the constraints are correct, thus disturbing the learning from grasping label.

4.3. Results on Contact-Score Joint Optimization

We employ the C-SJO in our 6-DoF grasp detection network trained with PCR and conduct ablations. The results

Model	Seen	Similar	Novel
No Refine	<u>66.67</u>	<u>65.55</u>	35.58
+ C-S (Predicted Mask)	66.61	65.37	36.67
+ C-S (GT Mask)	66.69	65.50	<u>36.61</u>
Original C-S	66.48	65.29	36.27
w/o C	66.65	65.64	35.86
w/o S	66.54	65.37	36.23

Table 2. Results of C-SJO on scenes captured by RealSense.

are shown in Table 2. We incorporate a recent proposed 3D segmentation method [38] to get object point-clouds from the clutter for optimization. With the ground-truth mask and segmented mask, C-SJO can improve by 1.03% and 1.00% on novel set separately. The C-SJO has almost no impact on the seen and similar set, primarily because the grasp poses predicted for seen and similar objects are sufficiently stable, making it challenging to find a better grasp than the original one. However, for the novel set, many unstable grasps exist that can potentially be optimized. We also conduct ablations about different designs of the C-SJO. Without the proposed projection contact map, only employing the original contact map (Original C-S) drops on seen, similar and novel set due to the singularity poses during optimization. Optimizing solely based on grasp score (w/o C) overlooks the contact map prior, resulting in very limited improvement on the novel set. Using only the contact map for optimization (w/o S) yields a 0.38% drop on the novel set, but the absence of grasp scores restricts the search space, making it challenging to locate the locally optimal grasp during the optimization process. The process of grasp pose optimization is shown in Fig. 5, where the optimal grasp poses are reached in the original grasps' neighbor $SE(3)$ space. For object (1)-(4), the optimization process refines the inaccurate initial grasp poses. For objects (5) and (6), the optimization process facilitates collision avoidance.

4.4. Comparison with State-of-the-art

To make a fair comparison with the state-of-the-art methods of the GraspNet-1billion benchmark, we re-implement

Model	Seen			Similar			Novel		
	AP	AP _{0.8}	AP _{0.4}	AP	AP _{0.8}	AP _{0.4}	AP	AP _{0.8}	AP _{0.4}
GraspNet-baseline [10]	28.10	30.53	26.56	23.87	26.92	22.51	7.48	8.43	4.93
Scale-balanced Grasp [19]	46.05	51.02	44.27	37.76	44.27	34.75	17.09	21.04	10.20
GSNet [35]	60.47	71.05	52.06	58.55	69.38	53.08	28.06	36.19	14.09
Ours Baseline	66.09	75.57	60.63	64.82	74.10	61.51	30.61	37.61	17.06
Ours	66.61	75.67	61.52	65.37	74.35	61.28	36.67	45.08	20.90

Table 3. Comparison with the state-of-the-art methods on RealSense scenes of GraspNet-billion benchmark.

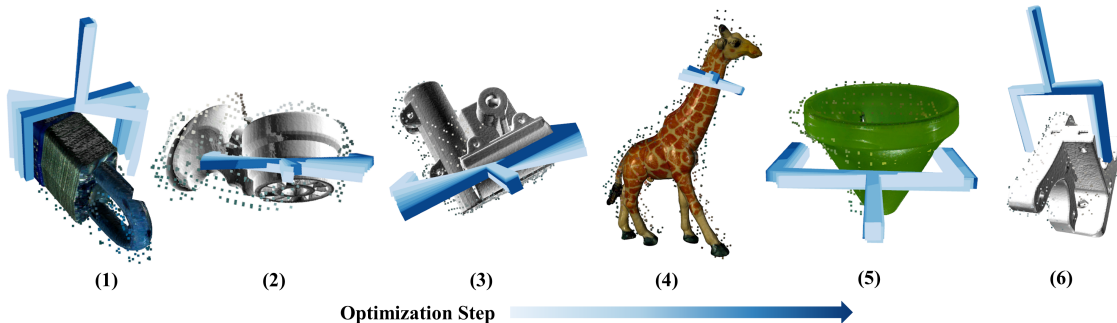


Figure 5. Visualization of the process of C-SJO.

three representative 6-DoF grasp detection methods [10, 19, 35] with our multi-view reconstructed scene as input. As shown in Table 3, our method performs better than previous 6-DoF grasp detection methods on all test sets and achieves 36.67% on the novel set, which demonstrates the generalization capability of our method.

4.5. Comparison with object augmentation

We give a comparison between our prior knowledge based method and the object augmentation which employed by previous methods to enhance the generalization capability. To migrate the procedural or learning-based object augmentation method on the GraspNet-1billion benchmark, since the similar objects and the training objects have similar distributions, we consider the similar set in the benchmark as objects obtained through the augmentation. We merge the two sets for joint training. In this way, we can conveniently validate the performance of data augmentation on this benchmark without the need to generate additional objects and annotate grasps. As shown in Table 4, introducing object augmentation can slightly improve the performance on seen and novel sets, benefiting from the richer object distribution. However, our method performs better on the novel set, improving by 4.37% compared to the object augmentation method, without introducing any additional data. Simultaneously, our method also exhibits an increase of 0.33% on novel set when paired with object augmentation, demonstrating that our method and object augmentation can be used together.

Model	Seen	Similar	Novel
Baseline	66.09	64.82	30.61
Augmentation	68.12	-	32.30
Ours	66.61	65.37	36.67
Ours + Augmentation	68.31	-	37.00

Table 4. Comparison with object augmentation.

4.6. Result Visualization

In figure 6, we visualized the results generated by the baseline method, object augmentation and our approach on the GraspNet-1billion benchmark. The gripper poses in red represent successful grasps, while those shown in purple and blue correspond to collision and bad grasps. By incorporating domain prior knowledge, our method can generate grasp poses that conform to the physical relationship between the gripper and the object. For objects (3)-(5), our method predicts some failed grasps, primarily due to poor grasp sampling locations or inaccurate perception of the object’s geometry.

4.7. Real-world Evaluation

The effectiveness of the proposed method in real-world is validated by real robot in this section. As shown in Figure 7 (a), the robotic grasping system is built on a 6-DoF UR-10 robot arm and a RealSense D435i depth camera is employed for scene perception. The total of 20 objects used for grasp-

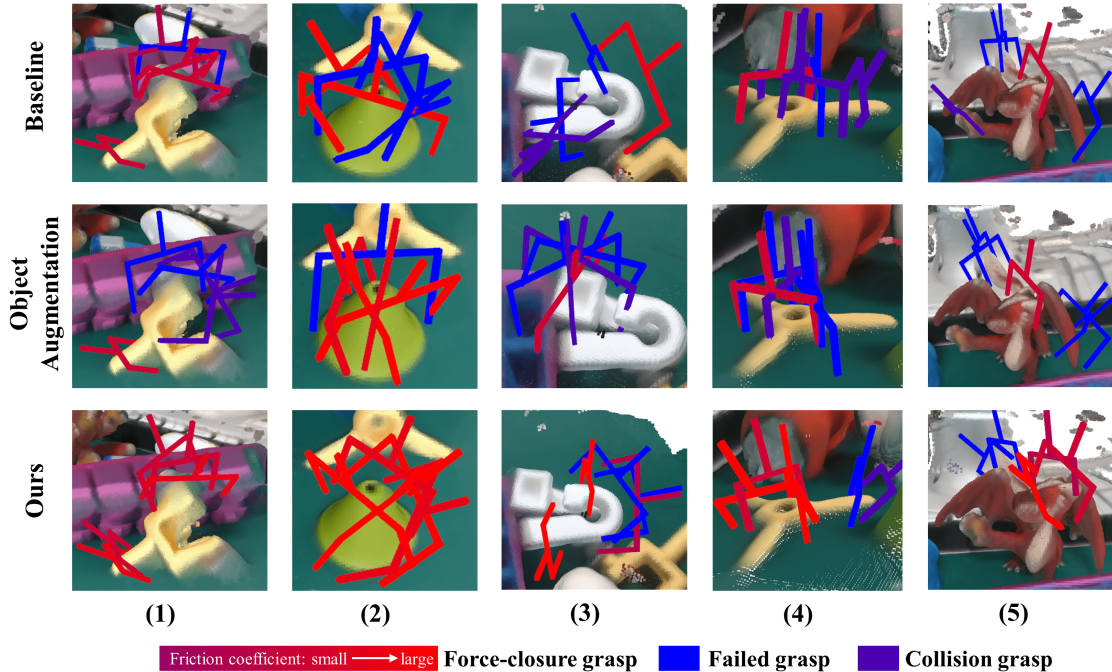


Figure 6. Visualization of the predicted grasp poses from baseline, object augmentation and the methods proposed in this paper.



Figure 7. (a) Robotic grasping system and (b) objects for real-world grasping.

ing (Fig. 7 (b)) are composed of two parts: 13 3D-printed objects from Dex-Net [20] and 7 objects chosen from the YCB dataset [4]. All of the objects are significantly different from the objects used for training in GraspNet-1billion. Before executing the proposed grasp detection method, we quickly reconstruct the scene using an arm-mounted depth camera based on the KinectFusion [25].

Model	Isolated	Cluttered	
	SR (%)	SR (%)	SCR (%)
Baseline	58.33 (35/60)	48.21 (43/89)	86.00 (43/50)
Ours	68.33 (41/60)	64.86 (48/74)	96.00 (48/50)

Table 5. Results of the real-world grasping experiments.

We compare our model to the baseline in two settings: isolated object grasping and cluttered object grasping. For isolated object grasping, each object is placed in three different poses and Success Rate (SR) is used as the metric.

For cluttered object grasping, we compose 5 objects into a scene and make the robot remove them all with a maximum number of operations at 10. SR and Scene Completion Rate (SCR) are employed as the metrics. As illustrated in Table 5, our model outperforms the baseline in both settings and achieves better SR and SCR, demonstrating its superiority for novel objects.

5. Conclusion

In this paper, we work for generalizing 6-DoF grasp detection with domain prior knowledge of robotic grasping. The physical constraint regularization based on physical rules is proposed to enable the generalization of objects with largely varied shapes and structures. To refine the unstable results predicted by network in cluttered scenarios, we specially design a contact-score joint optimization with the contact map prior, in which a projection contact map is utilized. Extensive experiments on both the benchmark and the real-world robot demonstrate the effectiveness of our method for novel objects.

Acknowledgment

This work is partly supported by the National Key R&D Program of China (2022ZD0161902), the National Natural Science Foundation of China (62022011), the Research Program of State Key Laboratory of Software Development Environment (SKLSDE-2023ZX-14), and the Fundamental Research Funds for the Central Universities.

References

- [1] Konstantinos Bousmalis, Alex Irpan, Paul Wohlhart, Yunfei Bai, Matthew Kelcey, Mrinal Kalakrishnan, Laura Downs, Julian Ibarz, Peter Pastor, Kurt Konolige, et al. Using simulation and domain adaptation to improve efficiency of deep robotic grasping. In *IEEE International Conference on Robotics and Automation*, 2018. 2, 3
- [2] Samarth Brahmabhatt, Cusuh Ham, Charles C. Kemp, and James Hays. Contactdb: Analyzing and predicting grasp contact via thermal imaging. In *IEEE Conference on Computer Vision and Pattern Recognition*, 2019. 2
- [3] Michel Breyer, Jen Jen Chung, Lionel Ott, Roland Siegwart, and Juan I. Nieto. Volumetric grasping network: Real-time 6 DOF grasp detection in clutter. In *Conference on Robot Learning*, 2020. 2
- [4] Berk Çalli, Arjun Singh, James Bruce, Aaron Walsman, Kurt Konolige, Siddhartha S. Srinivasa, Pieter Abbeel, and Aaron M. Dollar. Yale-cmu-berkeley dataset for robotic manipulation research. *International Journal of Robotics Research*, 36(3):261–268, 2017. 8
- [5] I-Ming Chen and Joel W. Burdick. Finding antipodal point grasps on irregularly shaped objects. *IEEE Transactions on Robotics and Automation*, 9(4):507–512, 1993. 3
- [6] I-Ming Chen and Joel W. Burdick. Finding antipodal point grasps on irregularly shaped objects. *IEEE Transactions on Robotics and Automation*, 9(4):507–512, 1993. 1
- [7] Christopher Choy, JunYoung Gwak, and Silvio Savarese. 4d spatio-temporal convnets: Minkowski convolutional neural networks. In *IEEE Conference on Computer Vision and Pattern Recognition*, 2019. 6
- [8] Qiyu Dai, Yan Zhu, Yiran Geng, Ciyu Ruan, Jiazhao Zhang, and He Wang. Graspnerf: Multiview-based 6-dof grasp detection for transparent and specular objects using generalizable nerf. In *IEEE International Conference on Robotics and Automation*, 2023. 2, 3
- [9] Amaury Depierre, Emmanuel Dellandréa, and Liming Chen. Jacquard: A large scale dataset for robotic grasp detection. In *IEEE/RSJ International Conference on Intelligent Robots and Systems*, 2018. 1, 2
- [10] Haoshu Fang, Chenxi Wang, Minghao Gou, and Cewu Lu. Graspnet-1billion: A large-scale benchmark for general object grasping. In *IEEE/CVF Conference on Computer Vision and Pattern Recognition*, 2020. 2, 5, 7
- [11] Carlo Ferrari and John F. Canny. Planning optimal grasps. In *IEEE International Conference on Robotics and Automation*, 1992. 3
- [12] Hanwen Jiang, Shaowei Liu, Jiashun Wang, and Xiaolong Wang. Hand-object contact consistency reasoning for human grasps generation. In *IEEE/CVF International Conference on Computer Vision*, 2021. 4
- [13] Junnan Jiang, Xiaohui Xiao, Fei Chen, and Miao Li. Learning grasp ability enhancement through deep shape generation. In *International Conference on Intelligent Robotics and Applications*, 2022. 2, 3
- [14] Zhenyu Jiang, Yifeng Zhu, Maxwell Svetlik, Kuan Fang, and Yuke Zhu. Synergies between affordance and geometry: 6-dof grasp detection via implicit representations. In *Robotics: Science and Systems*, 2021. 2, 3
- [15] George Em Karniadakis, Ioannis G Kevrekidis, Lu Lu, Paris Perdikaris, Sifan Wang, and Liu Yang. Physics-informed machine learning. *Nature Reviews Physics*, 3(6):422–440, 2021. 2
- [16] Hongzhuo Liang, Xiaojian Ma, Shuang Li, Michael Görner, Song Tang, Bin Fang, Fuchun Sun, and Jianwei Zhang. Pointnetgpd: Detecting grasp configurations from point sets. In *IEEE International Conference on Robotics and Automation*, 2019. 2
- [17] Min Liu, Zherong Pan, Kai Xu, Kanishka Ganguly, and Dinesh Manocha. Deep differentiable grasp planner for high-dof grippers. In *Robotics: Science and Systems*, 2020. 3
- [18] Tengyu Liu, Zeyu Liu, Ziyuan Jiao, Yixin Zhu, and Song-Chun Zhu. Synthesizing diverse and physically stable grasps with arbitrary hand structures using differentiable force closure estimator. *IEEE Robotics and Automation Letters*, 7(1):470–477, 2022. 3
- [19] Haoxiang Ma and Di Huang. Towards scale balanced 6-dof grasp detection in cluttered scenes. In *Conference on Robot Learning*, 2022. 2, 3, 6, 7
- [20] Jeffrey Mahler, Jacky Liang, Sherdil Niyaz, Michael Laskey, Richard Doan, Xinyu Liu, Juan Aparicio Ojea, and Ken Goldberg. Dex-net 2.0: Deep learning to plan robust grasps with synthetic point clouds and analytic grasp metrics. In *Robotics: Science and Systems*, 2017. 1, 8
- [21] Andrew T. Miller and Peter K. Allen. Graspit! A versatile simulator for robotic grasping. *IEEE Robotics & Automation Magazine*, 11(4):110–122, 2004. 3
- [22] Douglas Morrison, Juxi Leitner, and Peter Corke. Closing the loop for robotic grasping: A real-time, generative grasp synthesis approach. In *Robotics: Science and Systems*, 2018. 2
- [23] Douglas Morrison, Peter Corke, and Jürgen Leitner. Egad! an evolved grasping analysis dataset for diversity and reproducibility in robotic manipulation. *IEEE Robotics and Automation Letters*, 5(3):4368–4375, 2020. 2, 3
- [24] Arsalan Mousavian, Clemens Eppner, and Dieter Fox. 6-dof graspnet: Variational grasp generation for object manipulation. In *IEEE/CVF International Conference on Computer Vision*, 2019. 2
- [25] Richard A. Newcombe, Shahram Izadi, Otmar Hilliges, David Molyneaux, David Kim, Andrew J. Davison, Pushmeet Kohli, Jamie Shotton, Steve Hodges, and Andrew W. Fitzgibbon. Kinectfusion: Real-time dense surface mapping and tracking. In *IEEE International Symposium on Mixed and Augmented Reality*, 2011. 5, 8
- [26] Van-Duc Nguyen. Constructing force-closure grasps. *International Journal of Robotics Research*, 7(3):3–16, 1988. 2, 3
- [27] Nancy S. Pollard. Closure and quality equivalence for efficient synthesis of grasps from examples. *International Journal of Robotics Research*, 23(6):595–613, 2004. 1
- [28] Ran Qin, Haoxiang Ma, Boyang Gao, and Di Huang. RGB-D grasp detection via depth guided learning with cross-modal attention. In *IEEE International Conference on Robotics and Automation*, 2023. 2

- [29] Yuzhe Qin, Rui Chen, Hao Zhu, Meng Song, Jing Xu, and Hao Su. S4G: amodal single-view single-shot SE(3) grasp detection in cluttered scenes. In *Conference on Robot Learning*, 2019. 2
- [30] Máximo A. Roa and Raúl Suárez. Computation of independent contact regions for grasping 3-d objects. *IEEE Transactions on Robotics*, 25(4):839–850, 2009. 1
- [31] Alberto Rodriguez, Matthew T. Mason, and Steve Ferry. From caging to grasping. *International Journal of Robotics Research*, 31(7):886–900, 2012. 3
- [32] Andreas ten Pas, Marcus Gualtieri, Kate Saenko, and Robert Platt Jr. Grasp pose detection in point clouds. *International Journal of Robotics Research*, 36(13-14):1455–1473, 2017. 1, 2
- [33] Josh Tobin, Lukas Biewald, Rocky Duan, Marcin Andrychowicz, Ankur Handa, Vikash Kumar, Bob McGrew, Alex Ray, Jonas Schneider, Peter Welinder, et al. Domain randomization and generative models for robotic grasping. In *IEEE/RSJ International Conference on Intelligent Robots and Systems*, 2018. 2, 3
- [34] Laura Von Rueden, Sebastian Mayer, Katharina Beckh, Bogdan Georgiev, Sven Giesselbach, Raoul Heese, Birgit Kirsch, Julius Pfrommer, Annika Pick, Rajkumar Ramamurthy, et al. Informed machine learning—a taxonomy and survey of integrating prior knowledge into learning systems. *IEEE Transactions on Knowledge and Data Engineering*, 35(1):614–633, 2021. 2
- [35] Chenxi Wang, Haoshu Fang, Minghao Gou, Hongjie Fang, Jin Gao, and Cewu Lu. Graspness discovery in clutters for fast and accurate grasp detection. In *IEEE/CVF International Conference on Computer Vision*, 2021. 2, 3, 6, 7
- [36] David Wang, David Tseng, Pusong Li, Yiding Jiang, Menglong Guo, Michael Danielczuk, Jeffrey Mahler, Jeffrey Ichnowski, and Ken Goldberg. Adversarial grasp objects. In *IEEE International Conference on Automation Science and Engineering*, 2019. 3
- [37] Yinzhen Xu, Weikang Wan, Jialiang Zhang, Haoran Liu, Zikang Shan, Hao Shen, Ruicheng Wang, Haoran Geng, Yijia Weng, Jiayi Chen, Tengyu Liu, Li Yi, and He Wang. Unidexgrasp: Universal robotic dexterous grasping via learning diverse proposal generation and goal-conditioned policy. In *IEEE/CVF Conference on Computer Vision and Pattern Recognition*, 2023. 4
- [38] Yunhan Yang, Xiaoyang Wu, Tong He, Hengshuang Zhao, and Xihui Liu. Sam3d: Segment anything in 3d scenes, 2023. 6